

MEMS DEFORMABLE MIRRORS FOR ADAPTIVE OPTICS

Thomas Bifano, Raji Krishnamoorthy Mali
Dept. of Aerospace and Mechanical Engineering
Boston University, Boston, MA 02215.

Julie Perreault, Mark Horenstein
Dept. of Electrical and Computer Engineering
Boston University, Boston, MA 02215.

David Koester
MEMS Technology Applications Center, MCNC
3021 Cornwallis Road, RTP, NC 27709.

ABSTRACT

This paper describes the development of continuous and segmented deformable mirrors fabricated using surface-micromachining technology. Such mirrors have applications in adaptive optics imaging systems to correct phase aberrations in the optical path. Electrostatic actuators with 2 μm surface-normal stroke provide controlled deformation to the mirror surface. Results of electromechanical characterization of several deformable mirrors are presented. Real time correction of optical aberrations is demonstrated using a single mirror segment with closed-loop feedback control.

INTRODUCTION

MEMS based deformable mirrors have been investigated by several research groups as an inexpensive and high-performance alternative technology to more conventional piezoelectric deformable mirrors. Previous research has focused on continuous, bulk-micromachined modal mirrors [1,2] and surface-micromachined, piston-motion segmented mirrors [3]. Our research investigates the first continuous-membrane, zonal correctors to be fabricated using surface-micromachining techniques. We have also developed segmented mirrors (both piston and tip-tilt types) having fill factors of 95 to 98% which are much higher than previously demonstrated.

Figure 1 shows a schematic of three deformable mirror systems evaluated in our experiments. In each case, the mirror(s) are supported by multiple attachments to an underlying array of identical, fixed-fixed electrostatic actuators. These actuators provide precise control of the position of the mirror's attachment points in the surface-normal direction. The typical actuator is constructed from a 300 μm -square deformable membrane spaced at a 350 μm center-to-center distance from its nearest neighbors. Segmented mirrors capable of pure piston motion only have no inter-actuator coupling, allowing much simpler control algorithms in multi-actuator systems. However, they may exhibit undesirable diffraction due to the gaps between segments. Continuous mirrors offer the advantage of no diffraction, but a complicated control algorithm is required to address inter-actuator coupling. Segmented mirrors with tip-tilt motion are a hybrid design and permit matched optical phase at mirror segment edges.

Prototype actuators and mirror systems were first fabricated in a three-layer multi-user polysilicon foundry process offered by MCNC (MUMPS). [4]. A detailed study of

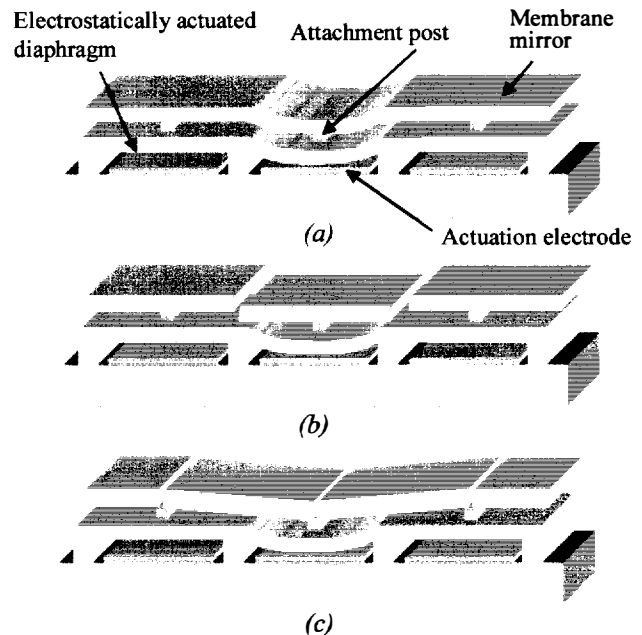


Figure 1. Schematic of deformable mirror array sections with (a) continuous mirrors (b) segmented mirrors with piston motion (c) segmented mirrors with tip-tilt motion.

electrostatic actuators fabricated in MUMPS reported previously [5], indicated a device yield that was sufficiently high (~95%) to make large-scale mirror arrays feasible. Statistical analysis of an ensemble of ramp actuation tests on these actuators revealed a position repeatability of 10 nm for σ limits corresponding to 99% probability. A dynamic motion response study showed the actuators to have a mechanical response frequency bandwidth greater than 70 kHz. However, some electrostatic charging effects were observed, possibly due to the presence of surface leakage paths [6].

Our early attempts to fabricate deformable mirrors using the MUMPS foundry process resulted in devices with excessive surface topography caused by patterning and etching of successive thin films. A novel planarization strategy based on setting a maximum line spacing for all patterned layers was developed and has enabled us to control surface topography to submicron levels. Restraining line spacing allows each deposited layer to fill in gaps as it conforms to the surface of the most recently deposited layer. Using this planarization strategy, we

have been able to fabricate mirrors with $0.75\ \mu\text{m}$ stroke capability, using the MUMPS foundry process. Experimental and modeling results for these mirrors have been previously reported [7].

The maximum line width planarization strategy also has been used to fabricate the mirrors described in this paper. Some print-through from underlying layers still occurs, but surface imperfections are limited to a fraction of a micron. In future designs, chemical mechanical polishing (CMP) of the final polysilicon layer will be added to eliminate this nanometer scale print-through.

FABRICATION AND TESTING OF MIRRORS

In our most recent set of experiments, prototype mirrors were fabricated using a custom, three-layer polysilicon surface micromachining process using polysilicon as the structural material, phospho-silicate glass (PSG) as the sacrificial material, and silicon nitride for electrical isolation of the actuators from the underlying substrate. Acid access for sacrificial release of the devices was provided by anisotropically etching holes in the substrate from the backside, thus avoiding holes in the mirror surface. Figure 2 shows the measured voltage-deflection curves for square actuators of various sizes. The usable range of deflection for these actuators before electrostatic pull-in occurs is $2\ \mu\text{m}$. Actuator motion was characterized using a single point displacement-measuring laser doppler interferometer.

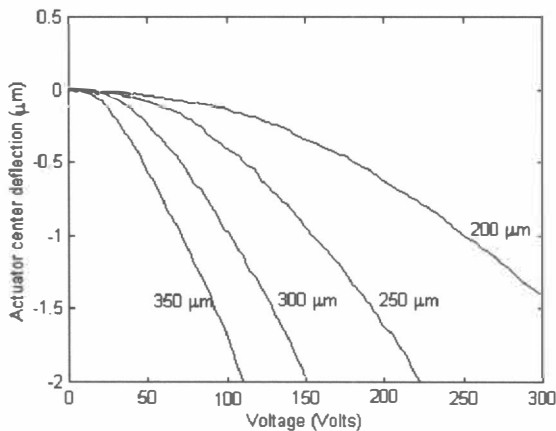


Figure 2. Measured deflection versus voltage for electrostatic fixed-fixed actuators.

An interferometric surface-mapping microscope (Phase Shift Technology MicroXAM) was used to map the surfaces of the mirrors. Figures 3(a) and 3(b) show a surface map measurement and cross-sectional surface profile of a continuous mirror supported by a 3×3 actuator array before deflection of any actuators. Figures 3(c) and 3(d) show the same surface maps after the deflection of the center actuator. Figure 4 shows the deflection of the mirror center versus voltage in response to a voltage ramp applied to the central actuator. Larger mirror arrays incorporating 100 and 400 actuators have also been fabricated in our experiments. Figure 5, for example, is a scanning electron micrograph (SEM) of a continuous mirror supported by 100 actuators.

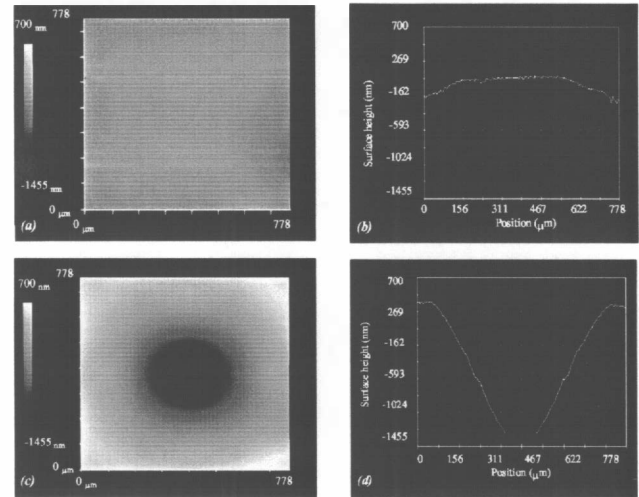


Figure 3. (a) and (b) show the surface map and x-profile through the center of a nine-element continuous mirror. (c) and (d) show the surface of the mirror when pulled down by the center actuator energized to 155 V. These measurements were made using an interferometric microscope.

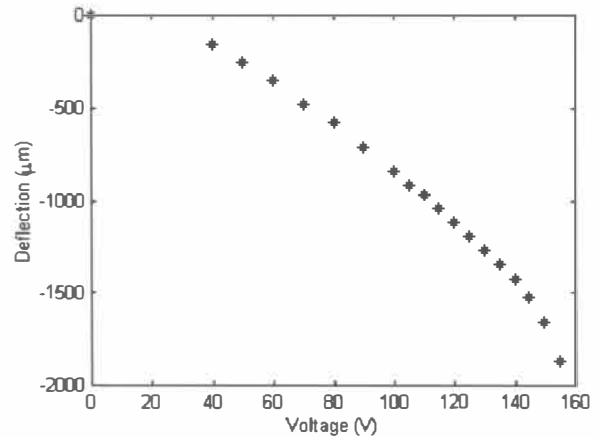


Figure 4. Response of a 3×3 actuator array supporting a continuous mirror membrane. Vertical actuator stroke is $2\ \mu\text{m}$.

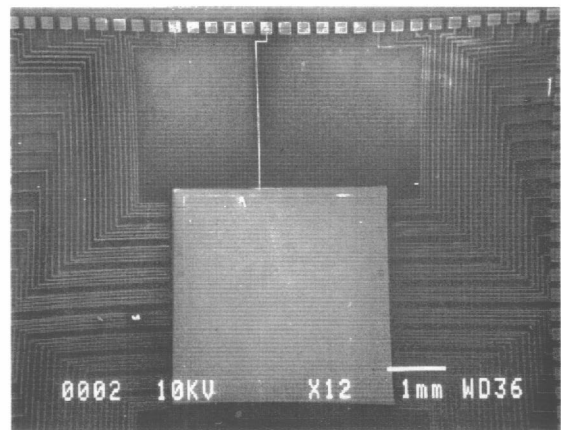


Figure 5. SEM micrograph of a 10×10 actuator array supporting a continuous mirror membrane.

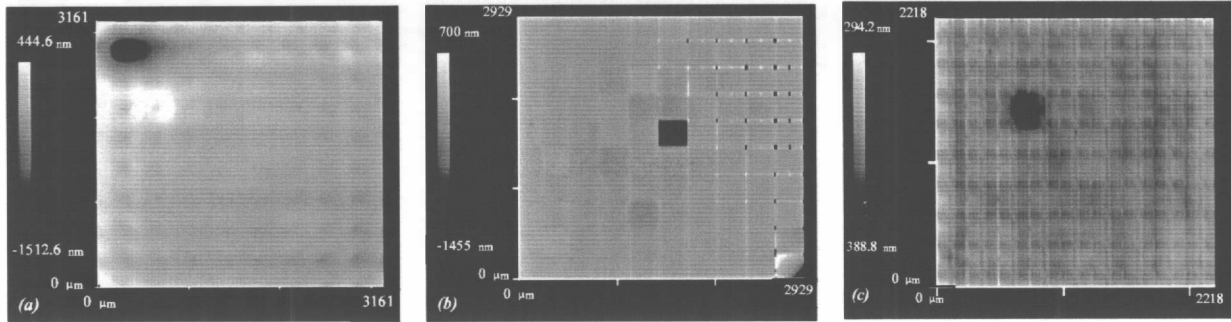


Figure 6. Interferometric surface maps of 10x10 actuator arrays with (a) continuous mirror (b) segmented mirrors with piston motion (c) segmented mirrors with tip-tilt motion. In each case a single actuator has been deflected.

Figure 6 shows interferometric surface maps of all three deformable mirror designs with local deflection caused by a single actuator. In these surface maps, darker color indicates that the surface has been pulled down. Note that significant coupling between actuators occurs in the continuous and hybrid tip-tilt mirrors because they are mechanically coupled through the mirror membrane. This coupling results in a smooth influence function in the neighborhood of the deflected actuator. In the case of the segmented piston mirror, no inter-actuator coupling occurs, resulting in sharp surface transitions at the boundaries of the actuated segment.

To evaluate the optical properties of the mirror, the local surface roughness of the polysilicon was measured using an atomic force microscope (Digital Instruments Dimension 3000). The peak-to-peak surface roughness was found to be 0.03λ , with an rms value of 0.007λ ($\lambda=633$ nm). Measurements also show post-release deformation of approximately $\lambda/6$ to $\lambda/2$ for various mirrors, depending on the size of the actuators used. This initial deformation is due to residual stresses and stress gradients in the thin film polysilicon, and is about 10% of the total available actuator stroke. The measured reflectivity of the polysilicon was approximately 50% at 633 nm. In future designs, a high reflective coating could be added to improve the reflectivity and optical efficiency of the mirrors.

ADAPTIVE OPTICS

In adaptive optics systems, deformable mirrors are used as active elements for phase aberration correction. Applications of AO systems include astronomy, medical imaging, and optical image correlation. The most common AO systems use nominally flat, deformable secondary mirrors whose shape is adjusted to compensate for aberrations in optical wavefronts. An aberrated incoming wave is sent to a wavefront sensor (e.g., a Hartmann sensor) which optically analyzes the wavefront for tilt and shape. The output of the wavefront sensor is used to produce “tilt” signals to control a tilt, or steering, mirror, and “shape” signals to control the surface of a deformable mirror. These control signals together generate a conjugate shape that corrects the aberration.

We have performed preliminary experiments to demonstrate the feasibility of using our MEMS deformable mirrors for optical wavefront correction. Figures 7 and 8 show the laboratory setup and results of an experiment in which a

collimated beam of light was focused on a 3x3 actuator array supporting a continuous mirror membrane of the type shown in Fig. 1(a). The collimated beam, derived from a 1mW HeNe laser, was reflected off the MEMS deformable mirror and projected into a far field image plane through a beamsplitter. Figure 8 shows the far-field intensity distribution of the beam as reflected off the mirror. When the central actuator is energized, pulling the mirror into a concave shape, it causes the focal point to be pulled closer to the mirror plane. As a result, the projected image of the beam diverges in the far field.

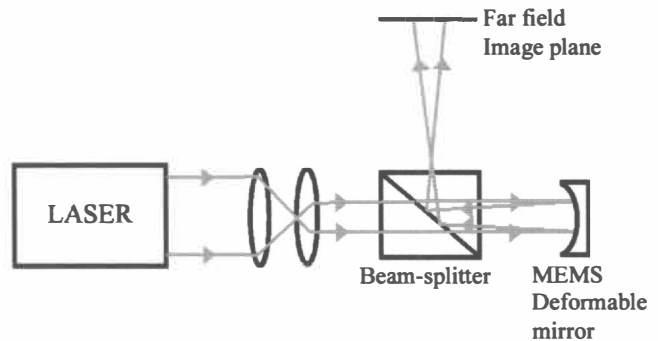


Figure 7. Schematic of experimental setup using the nine element mirror to focus a collimated laser beam.

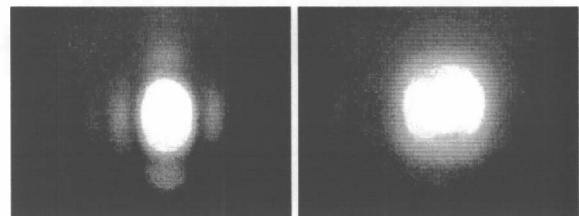


Figure 8. Measured far-field intensity distribution for plane wave reflected off of an (a) undeflected MEMS deformable mirror and (b) deflected MEMS mirror.

In a second experiment, we have implemented a real time closed loop controller capable of dynamically correcting aberrations in a laser beam. Figure 9 shows the experimental setup. A collimated 4 mW HeNe laser beam was focussed through a lens onto a single segment of a tip-tilt MEMS mirror array of the type depicted in Fig. 1(c). A dynamic aberration was introduced using warm air turbulence caused by a candle flame

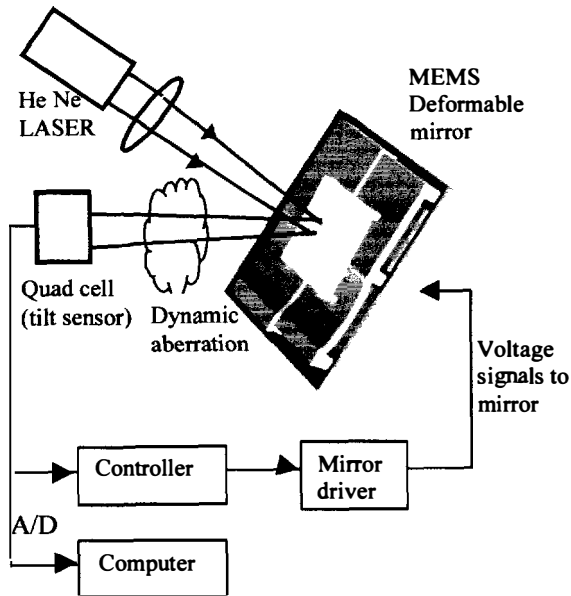


Figure 9. Schematic of experimental setup for real time control of wavefront tilt aberration.

near the beam. The wavelength of the aberration was much larger than the beam diameter, hence the effect of the aberration was to introduce a dynamic beam tilt. A quad cell photodetector was used to determine the centroid of the reflected beam along two orthogonal axes in the image plane. A quad cell contains four photodetectors, one in each quadrant, and integrates the energy in each quadrant to calculate the effective centroid of an incident beam. Two differential outputs from the quad cell (one for each axis) were fed into a closed-loop feedback circuit with proportional control. The control signals were amplified, added to an offset, and used to drive four actuators at the corners of a tip-tilt MEMS mirror segment. Because electrostatic actuators can only be pulled toward the substrate, an offset is required to permit both positive and negative tilt about an initial bias deflection.

Figure 10 shows measured wavefront tilt of the laser beam

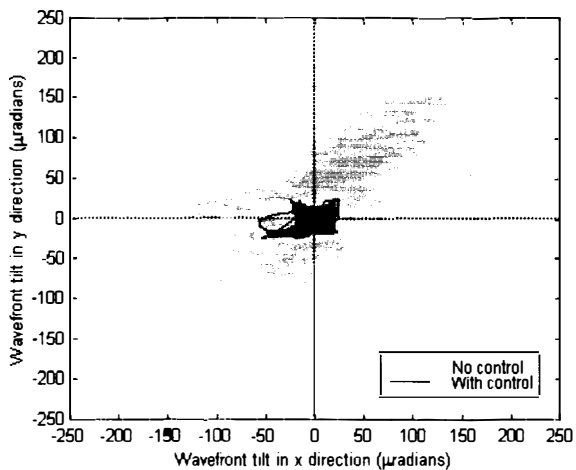


Figure 10. Random variations in two axis wavefront tilt measured by a quad cell photodetector, demonstrating correction of beam tilt.

along x and y axes (sampled at 2 kHz for 5 seconds). Grey corresponds to trajectories of beam tilt with the controller off, while the black corresponds to trajectories of beam tilt with the controller on. Significant reduction in beam tilt is evident the adaptive optics controller is activated.

DISCUSSION

Control of tilt using a single mirror segment demonstrates the fundamental operations needed to correct more complex wavefront aberrations. In an adaptive optics system based on a large array of MEMS actuators having many degrees of freedom, a Hartmann wavefront sensor, which is an array of lenslets, can be used to detect multiple wavefront aberrations. In such a system, local wavefront slopes translate into shifts in position of the individual focussed Hartmann spots. Detection of these spot shifts can be used to supply correction signals to the actuators of the mirror array.

ACKNOWLEDGMENTS

The authors would like to thank the Defense Advanced Research Projects Agency (DARPA) for funding this research project. Thanks are also due to Seth Pappas and Asaf Fishov for assistance with the control circuitry and Kendra Cermak for assistance with electromechanical characterization of actuators.

REFERENCES

1. G. Vdovin, P. Sarro, "Flexible mirror micromachined in silicon," *Appl. Optics*, 34 (1995), pp. 2968-2972.
2. Miller, M. Argonin, R. Bartman, W. Kaiser, T. Kenny, R. Norton, E. Vote "Fabrication and characterization of a micromachined deformable mirror," *Proc. SPIE 1945* (1993), pp. 421-430.
3. M. Roggemann, V. Bright, B. Welsh, S. Hick, P. Roberts, W. Cowan, J. Comtois, "Use of micro-electro mechanical deformable mirrors to control aberrations in optical systems: theoretical and experimental results," *Optical Engineering*, Vol. 36 no.2 (May 1997), pp. 1327-1338.
4. D. Koester, R. Mahadevan, K.W. Markus, "MUMPs Introduction and Design Rules", MCNC Technology Applications Center, 3021 Cornwallis Road, Research Triangle Park, NC, Oct. 1994. (<http://mems.mcnc.org/mumps.html>)
5. R. Krishnamoorthy Mali, T. Bifano, M. Horenstein, N. Vandelli, "Development of microelectromechanical deformable mirrors for phase modulation of light," *Optical Engineering*, Vol. 36 no. 2 (Feb. 1997), pp. 542-548.
6. M. Horenstein, T. Bifano, R. Krishnamoorthy Mali, N. Vandelli, "Electrostatic effects in micromachined actuators for adaptive optics," *Journal of Electrostatics*, 42(1-2), (Sep 1997).
7. T. Bifano, R. Krishnamoorthy Mali, J. Dorton, J. Perreault, N. Vandelli, M. Horenstein, D. Castañon, "Continuous membrane, surface micromachined, silicon deformable mirror," *Optical Engineering*, Vol. 36, no. 5, (May 1997), pp. 1354-1360.